Near Surface Geophysics

Near Surface Geophysics, 2018, **16**, 411–422 doi: 10.1002/nsg.12001

Investigating a firn aquifer near Helheim Glacier (South-Eastern Greenland) with magnetic resonance soundings and ground-penetrating radar

Anatoly Legchenko[1*], Clément Miège[2], Lora S. Koenig[3], Richard R. Forster[2], Olivia Miller[4], Douglas Kip Solomon[4], Nicholas Schmerr[5], Lynn Montgomery[3], Stefan Ligtenberg[6] and Ludovic Brucker[7,8]

[1]*Département Dynamiques Internes et de Surface des Continents (DISCO - IGE),University Grenoble Alps, Institute of Research for Development, CS 40700, 38 058 Grenoble Cedex 9, France,* [2]*Department of Geography, University of Utah, 332 1400 E, Salt Lake City, UT 84112, USA,* [3]*National Snow and Ice Data Center, University of Colorado, 216 UCB, Boulder, CO 80309, USA,* [4]*Department of Geology and Geophysics, University of Utah, Frederick Albert Sutton Building, 115 S 1460 E #383, Salt Lake City, UT 84112, USA,* [5]*Department of Geology, University of Maryland, 8000 Regents Dr., College Park, Maryland 20742, USA,* [6]*Institute for Marine and Atmospheric research Utrecht (IMAU), Utrecht University, P.O. Box 80000, 3508 TA Utrecht, The Netherlands,* [7]*Cryospheric Sciences Laboratory, Earth Science Division, Science and Exploration Directorate, NASA Goddard Space Flight Center, 8800 Greenbelt Rd, Greenbelt, MD 20771, USA, and* [8]*Goddard Earth Sciences Technology and Research Studies and Investigations, Universities Space Research Association, NASA Goddard Space Flight Center, Building 33, H102, Greenbelt, MD 20771, USA*

Received September 2017, revision accepted February 2018

ABSTRACT

We apply the magnetic resonance sounding (MRS) method to investigate a firn aquifer in the south-east region of the Greenland ice sheet. Our study aims to delineate and estimate the volume of the recently discovered water stored within the firn (compacted snow) that remains liquid throughout the year. We develop and test successfully a methodology for joint use of MRS and ground-penetrating radar (GPR). This non-invasive geophysical approach is particularly well-adapted to glacier conditions and has a promising future for *in situ* investigation of water distribution in glaciers. At our field site, MRS showed an aquifer located at variable depths between 20 and 30 m beneath the ice-sheet surface. At the monitoring site, both MRS and GPR show an increase in the water volume stored between April 2015 and July 2016. MRS estimates suggest that the volume increased by approximately 28%.

Key words: Greenland, glacier, meltwater, GPR, MRS.

INTRODUCTION

The recent discovery by Forster *et al.* (2014) of a non-freezing firn aquifer in the Greenland ice sheet posits questions regarding hydrology and water storage capacity of such a system. Firn aquifers represent a previously neglected component of the Greenland englacial hydrologic system that could store a significant amount of water, representing a potential sea-level rise of 0.4 mm (Koenig *et al.* 2014). Increasing air temperature over the Arctic regions may cause these spatially extensive aquifers to expand towards higher altitude and to become thicker, thus increasing the volume of stored water. This presence of water in the firn challenges our current understanding of the surface-meltwater routing through the ice sheet and affects both mass balance and sea-level rise estimates, as the aquifer could act as a temporary storage system buffering water run-off (Rennermalm *et al.* 2013; Miège *et al.* 2016). *In situ* measurements may contribute to better estimates of the water volume fluctuations within the firn, thus they are crucial to improve our understanding of the dynamics of water routing through the firn as well as the mechanisms of water discharge from the Greenland ice sheet to the ocean.

*E-mail: anatoli.legtchenko@ird.fr

Difficult measuring conditions and often heterogeneous subsurface encourage the use of non-invasive geophysical methods for investigating glaciers. Hoekstra (1978) reports electromagnetic methods applied to mapping shallow permafrost and Kneisel (2004) successfully uses two-dimensional (2D) resistivity imaging. The use of radar and seismic wave velocities for estimating englacial water content further extends the geophysical toolbox (Endres *et al.* 2009). Ground-penetrating radar (GPR) is probably the most popular geophysical tool applied to the investigation of glacier geometry (e.g. Arcone, Lawson and Delaney 1995; Rippin *et al.* 2003) and water distribution in ice formations (Murray *et al.* 1997; Moran *et al.* 2000; Bradford and Harper 2005; Irvine-Fynn *et al.* 2006). Analysis of GPR backscattering from Arctic glaciers (Björnsson *et al.* 1996; Murray *et al.* 2000; Pettersson *et al.* 2003) and GPR measurements near boreholes (Gusmeroli *et al.* 2010) shows that this method is also sensitive to the interface between cold and temperate ice (Irvine-Fynn *et al.* 2011). The surface nuclear magnetic resonance method also known as the magnetic resonance sounding (MRS) is selectively sensitive to subsurface liquid water, thus allowing unambiguous interpretation of field data in terms of groundwater identification (Semenov *et al.* 1989). This is the main advantage of MRS compared to other surface geophysical tools (seismic, gravity, electrical and electromagnetic methods). Several authors report successful use of MRS in a glacial environment (Lehmann-Horn *et al.* 2011; Nuber *et al.* 2013; Parsekian *et al.* 2013). Vincent *et al.* (2012) and Legchenko *et al.* (2014) report application of MRS in a 3D configuration for monitoring water accumulation in the Tête Rousse glacier. These reported results suggested combining MRS and GPR methods as one geophysical tool.

We focus our attention on MRS because it can reliably identify the presence of liquid water in ice and allows estimation of the water volume in the subsurface. However, MRS also comes with some disadvantages. First, the vertical resolution of the method is limited and progressively degrades with depth. The uncertainty in the depth resolution increases from 1 to 2 m close to the surface to more than 10 m at greater depth as defined by the system configuration. Practical implementation of MRS is complex and measurements are time-consuming; MRS requires deployment of heavy cables and multiple hours of monitoring. In comparison with MRS, GPR is not able to easily estimate the volume of water in ice, but GPR has a high spatial resolution (meters) and high production rate. Scan rates of 10–100 Hz are typical GPR features. Reflections of electromagnetic waves are due to changes in the dielectric constant of a given medium. Consequently, reflections are not only caused by the presence of water in ice, but also by ice lenses in the firn and changes in firn/ice density, thus, rendering interpretation of GPR measurements challenging in regard to extracting the water component of the signal. The first tentative joint use of MRS and GPR in the Arctic (Hansbreen glacier in Wedel Jarlsberg Land at Spitsbergen, Svalbard) is reported by Turu (2012). However, due to difficult measuring conditions, this survey had uncertain results. Vincent *et al.* (2012) and Garambois *et al.* (2016) report their experience from the French Alps. An englacial cavern in the Tête Rousse glacier has been detected and accurately located with GPR. Then, the volume of water in the cavern was estimated with MRS. The cavern was drained and the volume of water pumped from this cavern was found in a good agreement with that estimated with MRS. In this paper, we describe the method and present the results of our study, followed by a brief discussion on the remaining challenges.

METHOD

Magnetic resonance sounding

The nuclear magnetic resonance (NMR) phenomenon is a common tool used in physics, chemistry, medicine and geophysics. The capacity of atomic nuclei to absorb and transmit electromagnetic energy of a specific frequency, which is different for different nuclei, renders this phenomenon selectively sensitive to different types of material. NMR is reported to be an efficient tool for investigating water in ice and permafrost samples (Callaghan *et al.* 1999; Brown *et al.* 2012; Brox *et al.* 2015). The magnetic resonance sounding (MRS) method is a geophysical application of the NMR phenomenon employing hydrogen nuclei (H_1) in water molecules. Solid material containing H_1 produce much shorter NMR signals and, consequently, ice is undetectable with an MRS instrument tuned to liquid water that is characterized by signals with a relatively long relaxation time. The resonance behavior of proton magnetic moments in the earth's magnetic field ensures that the method is sensitive only to groundwater. Thus, the MRS is a non-invasive geophysical technic developed for groundwater investigation. In the 1D configuration, this method allows investigating laterally homogeneous water-saturated formations (Legchenko and Valla 2002). In this case we assume that the subsurface is horizontally stratified, and MRS results provide a vertical distribution of the water content. Recently developed 2D (Boucher *et al.* 2006; Hertrich *et al.* 2007, 2009; Legchenko *et al.* 2011a) and 3D methodology (Legchenko *et al.* 2011b;

Chevalier *et al.* 2014; Jiang *et al.* 2015) allows investigating with MRS complex and heterogeneous subsurface structures.

For performing MRS measurement, we generate a pulse of alternating electrical current in the surface loop. The pulse moment $q=I_0\tau$ is as a product of the current amplitude I_0 and the pulse duration τ. One sounding consists of measuring the amplitude of the MRS signal (e_0) with different values of the pulse moment. The frequency of the current is equal to the resonance frequency for hydrogen nuclei in the geomagnetic field (Larmor frequency). We obtain the Larmor frequency $\omega_0=\gamma B_0$ from measurements of the geomagnetic field (B_0) on the surface, where γ is the gyromagnetic ratio for hydrogen ($\gamma/2\pi = 4.258 \times 10^7$Hz/Tesla). In the 1D implementation, we assume the subsurface horizontally stratified and compute the amplitude as

$$e_0(q) = \frac{\omega_0}{I_0}\int_z B_\perp(z)M_\perp(z)w(z)dz, \tag{1}$$

where $B_\perp$ is the transversal to the geomagnetic field component of the loop magnetic field, $M_\perp=M_0\sin(0.5\gamma B_\perp\tau)$ is the transversal component of the nuclear magnetization with M_0 being the macroscopic nuclear magnetization and $0 \le w(z) \le 1$ is the water content in the subsurface.

We assume the horizontal stratification and approximate equation (1) by a system of algebraic equations (Legchenko and Shushakov 1998)

$$\mathbf{Aw} = \mathbf{e}_0, \tag{2}$$

where $\mathbf{A} = [a_{i,j}]$ is a rectangular matrix of $I \times J$, $\mathbf{e}_0 = (e_{01}, e_{02}, \dots, e_{0i}, \dots, e_{01})^T$ is a set of experimental data, $\mathbf{w} = (w_1, w_2, \dots, w_j, \dots, w_J)^T$ is a vertical distribution of the water content. Thus, MRS allows estimating the volume of water per surface unit as

$$V_{\text{water}} = \sum_{j=1}^{J}(w_j \times \Delta z_j), \tag{3}$$

where w_j and ΔZ_j are the water content and thickness of each layer j of the inverse model.

MRS inversion is ill-posed, and many different approaches to resolution of the MRS inverse problem have been reported (Guillen and Legchenko 2002a,b; Mohnke and Yaramanci 2002; Braun and Yaramanci 2008; Grombacher *et al.* 2017). For resolving equation (2), we use one of the most popular inversion schemes based on the Tikhonov regularization method (Tikhonov and Arsenin 1977; Morozov 1966). For getting the optimal solution, this method utilizes minimization of a Tikhonov functional $M(\eta)$

$$M(\eta) = \left\| \mathbf{Aw} - \mathbf{e}_0 \right\| L_2 + \eta \left\| \mathbf{w} \right\| L_2, \tag{4}$$

where $\eta>0$ is called the regularization parameter. Regularization acts as a filter for getting a smooth solution. $M(\eta)$ has a unique minimum and hence provides the unique solution (optimal in the Tikhonov formulation), which is a trade-off between the fitting error and smoothness of the solution shape.

The resolution of the MRS inverse problem depends on measurement conditions and can be investigated for each particular data set using different mathematical methods. For example, Müller-Petke and Yaramanci (2008) report the use of the singular value decomposition (SVD). Guillen and Legchenko (2002a) use the Monte Carlo simulations. For this work, we estimate the resolution by computing the model resolution matrix using the SVD. We select the number and the thickness of the model layers in matrix **A** (equation (2)) so that the model resolution matrix becomes the identity matrix (Legchenko and Pierrat 2014). We consider the field setup used in Greenland (a coincident Tx/Rx square loop with 80-m sides and a maximum pulse moment of 3000 A·ms) and assume a low-noise close to the threshold of the MRS instrument (10 nV). Under these assumptions, we estimate the maximum depth of detection of a 10-m-thick layer with 5% of the water content at approximately 68 m (top of the layer). Then, we calculate the minimum thickness of the model layers that can be resolved between 0 and 80 m (Legchenko *et al.* 2017).

Figure 1 shows that MRS has a resolution of about 0.5 m close to the surface. At 20 m, the resolution is about 10 m, and it degrades progressively with increasing depth. A more detailed presentation of the method may be found in the review papers (Hertrich 2008; Behroozmand *et al.* 2015) and in a textbook (Legchenko 2013).

Ground-penetrating radar

In order to obtain the depth to the water table using ground-penetrating radar (GPR) data, the conversion of the two-way travel time (TWT) to depth is required. For that, we consider snow and firn as a non-magnetic and low-loss dielectric medium and approximate electromagnetic wave velocity (v) as

$$\text{v} = c/\sqrt{\varepsilon\prime}, \tag{5}$$

where $c = 0.3$ m/ns is the velocity in a vacuum and ε' is the dielectric permittivity of the medium. The dielectric permittivity versus depth was set based on the empirical

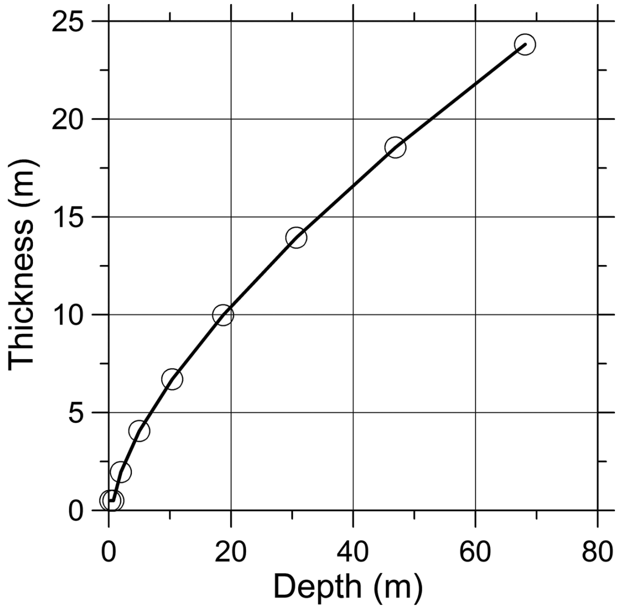

Figure 1 The minimum thickness of the model layers that can be resolved versus layer depth estimated with the singular value decomposition (SVD) and considering the measuring set-up and conditions in Greenland.

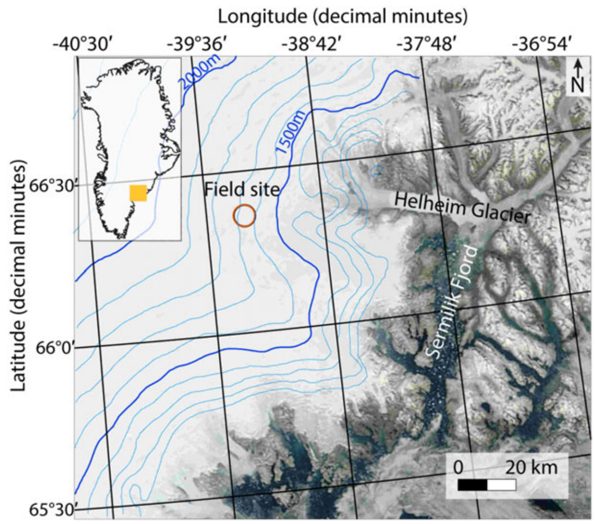

Figure 2 Location of the area investigated with MRS in Greenland projected on the background image from NASA Terra MODIS sensor (image taken on 19 July 2015) and elevation contours from Cryosat-2 digital elevation model (Helm *et al.* 2014).

relationship associating it to the snow/firn density profile ($\rho(z)$) from Kovacs *et al.* (1995):

$$\varepsilon\prime = (1 + 0.845\rho(z))^2. \tag{6}$$

Smoothing the density profile versus depth allows minimizing the impact of small-scale spatial density heterogeneities in the firn as, for example, ice lenses and ice columns.

INVESTIGATED AREA

The study area is located in S–E Greenland (Figure 2). Our field site is a part of the lower portion of the accumulation zone (also known as the percolation zone) of the ice sheet and is located about 50 km West of Helheim Glacier terminus. According to regional climate model simulations averaged over 1979–2014 (Fettweis *et al.* 2013), this region witnesses high-averaged snow accumulation rates of 1.46 m of the water equivalent per year (w.eq. y^{-1}) during the winter and spring times and averaged moderate to high melt rates in summer of 0.61 m w.eq. y^{-1}. Additional GPR profiling combined with firn-core depth-age scales confirmed the modeled high snow accumulation of this region (Miège *et al.* 2013). We focussed our study on this area because the airborne radar data recorded annually (in April–May) as part of NASA Operation IceBridge since April 2010 showed persisting firn-aquifer conditions (Miège *et al.* 2016). Based on seismic measurements performed simultaneously to the MRS and GPR observations, we find the ice thickness is approximately 800–1000 m (Montgomery *et al.* 2017). In order to study the ice dynamics, we maintained stationary GPS receivers over a period of a few days. The derived surface displacement velocity was 30–40 cm/day with an average direction towards the glacier terminus.

We carry out the MRS survey in Greenland using NUMIS$^{\text{LITE}}$ MRS System fabricated by IRIS Instruments (http://www.iris-instruments.com/), which allows non-invasive imaging of water distribution down to approximately 60–80 m. For all measurements, we use a square loop with 80-m sides. Measuring time is between 2.5 and 3.5 hours per station. Under Greenland conditions, installation of the measuring loop by two persons takes about 1 hour, sometimes longer. We observed the noise level between 100 and 150 nV, which allows high-quality measurements. With 100 stacks, noise is reduced to approximately 5 nV with the MRS signal varying between 10 and 160 nV.

For performing GPR measurements, we use the common-offset survey with a commercial GPR instrument from Geophysical Survey Systems, Inc.© (http://www.geophysical.com/) outfitted with a 400 MHz antenna. The data set is composed of 2048 samples per trace with a sample interval of 0.24 ns. It allows us to achieve a TWT vertical range of 500 ns. The sampling rate is variable with an average of six scans per second. With the GPR controller installed on a snowmobile towing the radar antenna on a sled, we obtain an average trace spacing of 0.5 m, driving about 10 km h^{-1}. For improving data quality, we use a time-dependent gain and stacking. The post-processing is composed of adjustment for time zero, application of filters for improving the visual display and geolocation of the GPR profile using GPS data. For that, we use a Trimble R7© GPS with a sampling interval of 5 s or ~15 m. We process GPS data using precise point positioning service hosted by the online Canadian Spatial Reference Service. Miège *et al.* (2016) present more details about the use of GPR under Greenland conditions.

GPR and MRS equipment are portable into the field. We transport boxes from the base camp to the ice sheet via sling-loading beneath a helicopter. We then installed the GPR on the snowmobile and carried the MRS equipment with a sled (Figure 3).

RESULTS

At one location (MRS6 station), we have three time-lapse measurements (24 April 2015, 31 July 2015 and 27 July 2016). It allows us to follow the evolution of the water volume stored in the firn during the summer 2015 and an annual variation of the water storage between July 2015 and July 2016. We compare magnetic resonance sounding (MRS) with borehole and ground-penetrating radar (GPR) measurements corresponding to the same period (Figure 4). MRS inversion for the water content provides a vertical distribution of water in the firn, which allows estimation of the depth and thickness of the water-saturated formation. When applied in rocks, the relaxation times of the MRS signal (T_1, T_2^* and T_2) allow estimation of the mean grain-size of the water-saturated formation. However in ice, snow and firn, the relaxation times are long even in the unsaturated zone (during our study we observed $T_2^* > 300$ ms for all soundings) and, consequently, the pore-size information contained in MRS results is poor. In our work, we neglected it as a parameter, which has no effect on the water volume estimate. Boreholes provide the depth to the water table and the thickness of the aquifer from the firn core analysis consisting of core density measurements and visual observation of stratigraphy changes (Koenig *et al.* 2014). GPR allows estimation of the depth to the water table and its spatial variations (e.g. Forster *et al.* 2014). In April 2015, MRS observations show the water table at a depth of ~20 m below the ice-sheet surface with the water table measured in the borehole at 19.7 m. This result is in a good agreement with the density profile, which shows a sharp density increase at this depth. The density increase is due to the transition from unsaturated to saturated firn (Koenig *et al.* 2014). Both MRS and the core analysis show the bottom of the aquifer as it represents a gradual change from saturated firn to solid ice due to slow refreezing. MRS resolution is limited (Figure 1), which does not allow accurate determination of the bottom of the aquifer located at approximately 30 m. The density measurements also do not provide sufficient accuracy for reliably detecting the density difference between the water-saturated firn and solid ice. Therefore, we complemented the density measurements with observation of visual stratigraphy changes from water-saturated firn to solid ice, which allowed us to improve our estimation of the aquifer bottom depth. The core visual analysis suggests the bottom at approximately 33–35 m. In 2016, GPR shows the water table higher compared with that observed in April 2015. MRS also shows an increase in the water volume in April 2015 (0.77 m^3 m^{-2}) compared to 0.98 m^3 m^{-2} observed in July 2016, thus supporting the GPR results. These observations suggest that the volume of water stored in the firn is increasing.

During our fieldwork, we used the MRS field set-up optimized for investigating the aquifer, but the unsaturated firn and, consequently, details of the water distribution in the shallow part of the unsaturated firn column are not well resolved. However, measurements in July 2015 and July 2016 show more water in the first 7 m of the subsurface than observed in April 2015 (Figure 4a). These observations are consistent with the intensive summer melt in July and the pre-melt conditions observed in April when the surface temperature in in this area is below 0°C (Koenig *et al.* 2014). Shallow water revealed by MRS may cause reflections observed in the summer GPR profiles. However, we also observed similar reflections in drier and colder firn. GPR surveys, done before the surface melt onset, suggest that these reflections may be due to density contrast and the presence of laterally extensive ice lenses in the firn (e.g. Christianson *et al.* 2015; Miège *et al.* 2016), making it difficult to relate them exclusively to the presence of water.

Measured amplitude of the MRS signal is directly proportional to the volume of water in the subsurface and is the most objective parameter provided by MRS. Such a comparison is particularly reliable for time-lapse measurements. Note that the amplitude of the MRS signal depends on the size of the measuring loop and, consequently, we can compare directly measurements carried out with the loop of the same size. The wire cross-section of the loop and small variations in the loop shape have minor effect on the MRS signal. We verify the instrument each time before starting fieldwork and after returning to the office by measurements at the test site in France with

Figure 3 GPR system ready for data collection on the glacier (left) and MRS instrument prepared for measurements (right). Photographs taken by Clément Miège.

known MRS response. Figure 5a shows the MRS amplitude versus pulse moment observed in Greenland at the monitoring site in 2015 and 2016. We use the same loop and the same instrument. Observed increase in the amplitude of the MRS signal confirms the increase in the water volume shown by MRS (Figure 5b). In April 2015, difficult weather conditions limited helicopter ground time (and, consequently, fieldwork time), which caused the volume estimate less accurate.

Figure 6 shows a comparison of the water content provided by MRS projected on a GPR profile. We observe a good correlation between the measurements. For example, stations MRS7 and MRS8 show very low water content in the areas where GPR does not show a reflected signal associated with the top of the aquifer.

Figure 7 shows the MRS-estimated depths to the top of aquifer with that inferred from GPR. Circles show the water static level measured in boreholes. We observe a generally good correspondence between these different technics.

However, the correspondence between the water table locations obtained by these different technics is not perfect. Measurements reveal some dispersion that is caused by different factors. Indeed, when the structure of firn is heterogeneous, multiple reflections in the GPR data may make it challenging to identify which reflection corresponds to the water table. MRS estimates of the water content are averaged over the loop surface and GPR provides results along a linear profile. Measurements in borehole are accurate but focussed on the well. The scale factor may also cause additional uncertainty while using the 1D measurements in the 3D environment. For demonstration, Figure 8 shows an example of GPR measurements with multiple reflections.

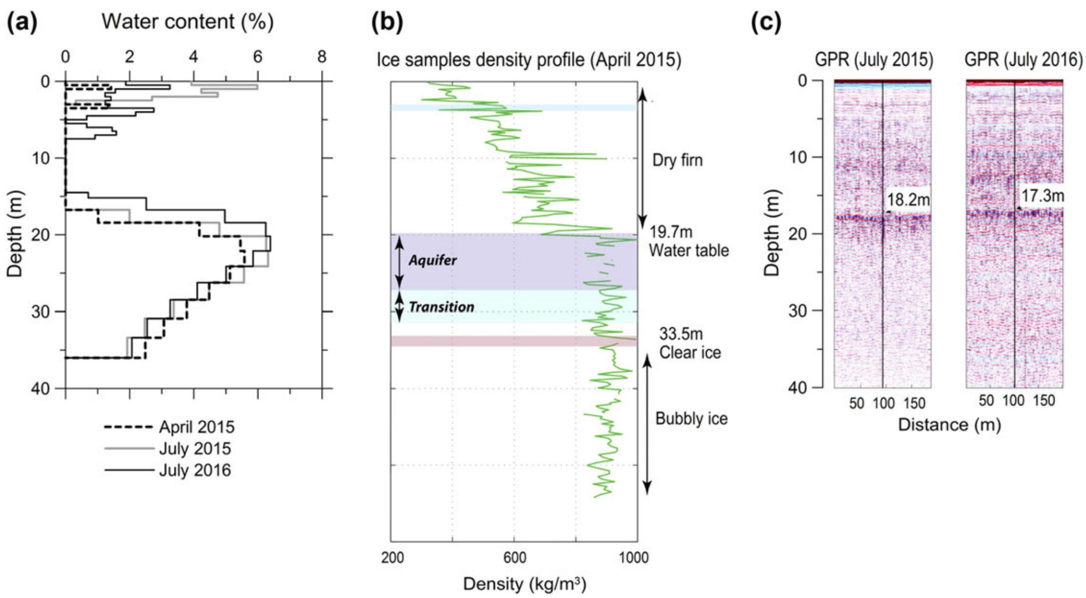

Figure 4 Comparison of three time-lapse MRS soundings with borehole and GPR results: (a) a vertical distribution of the water content derived from MRS measurements; (b) the ice core density log from borehole at the location of the MRS station in April 2015; and (c) GPR cross-sections measured in July 2015 and July 2016 across the MRS loop. The vertical depth axis for all three panels is identical.

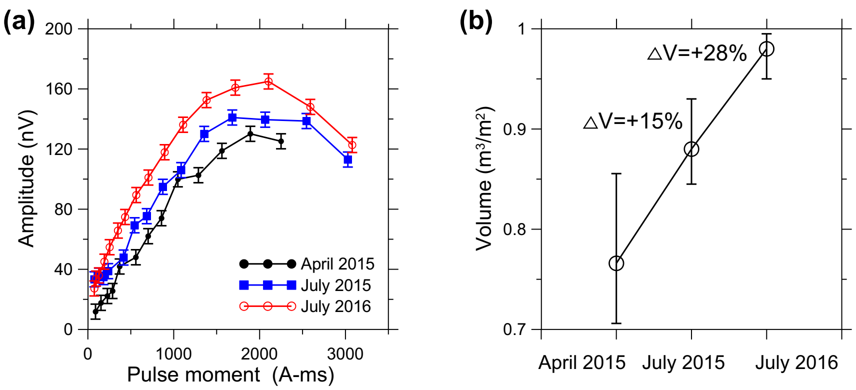

Figure 5 (a) Measured amplitude of the MRS signal versus pulse moment for the same station in 2015 and 2016; (b) the volume of water per surface unit estimated with MRS. DV shows evolution of the water volume observed in July 2015 and 2016, relative measurements in April 2015.

DISCUSSION

Magnetic resonance sounding (MRS) results show an increase in the water volume stored in the firn observed between April 2015 and July 2016. However, precise quantification of stored water is a challenging task with any available method that merits additional discussion. We mainly face two types of difficulties: one relates to a limited accuracy of the available geophysical methods, and the other relates to the complexity of the ice–firn–water system instability around 0°C.

Reported in the literature measurements of the density of ice samples extracted from borehole allow estimates of the water content based on the density difference between ice, water and air (Koenig *et al.* 2014). We assume the air density to be 0 kg m^{-3} and it can be neglected. The density of ice is 916.7 kg m^{-3} at 0°C, whereas water has a density of 999.8 kg m^{-3} at the same temperature. Weighting samples of known volume would lead to a water content estimate. For example, Figure 4b shows that the smaller density of the unsaturated firn samples allows reliable detection of the water table. However, the difference between cold ice and water-saturated firn at the depth below 30 m is small, which renders detection of the aquifer bottom more difficult. To illustrate this point, we calculate the density of ice with 5%

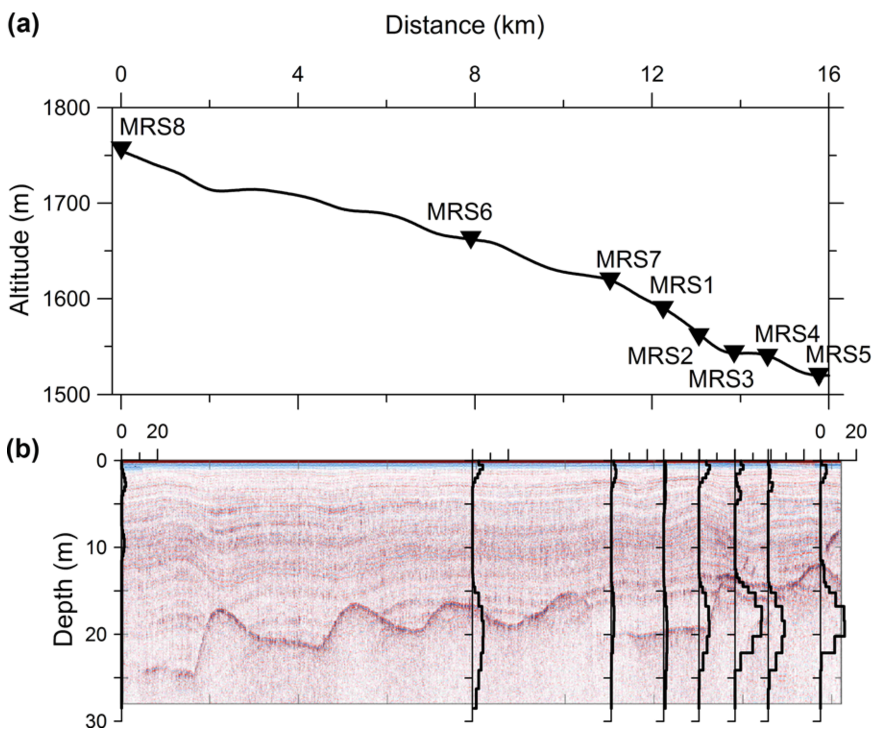

Figure 6 Comparison of MRS and GPR results obtained in 2015: (a) location of MRS stations along profile; (b) MRS water content (%) versus depth for all soundings projected on a GPR profile. Topography is not removed from the GPR profile.

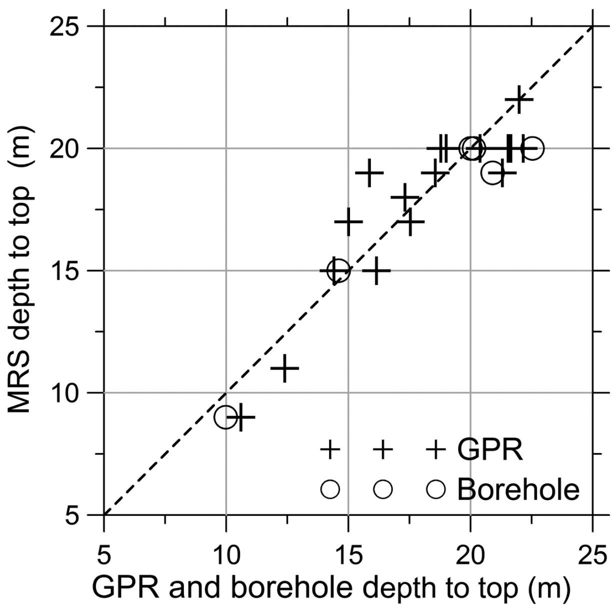

Figure 7 MRS estimated depth to the top of aquifer versus that obtained from GPR measurements and the static water level measured in boreholes.

of water and compare it with the sample containing 20% of water. Assuming no air in the samples, we obtain 920.9 and 933.3 kg m^{-3}, respectively. Therefore, for distinguishing between these samples, we need measurements with the uncertainty better than (933.3 − 920.9) = 12.4 kg m^{-3}, which represents the relative uncertainty of 12.4/933.3 = 1.3%. In practice, it is difficult to keep the water in the firn core from escaping or refreezing during extraction and, consequently, to get such an accuracy under field conditions is challenging.

Ground-penetrating radar (GPR) provides an accurate measurement of the travel time between transmitted pulses and received reflections. The arrival time is then converted into the depth to each reflector. Accuracy of this conversion requires development of an accurate velocity model. Equation (5) shows that the velocity **v** is strongly dependent on the real part of the dielectric constant (permittivity) of the medium ε', which in turn is strongly dependent on the water content (e.g. Murray *et al.* 2007). Thus, the seasonal routing of water in the firn may affect the accuracy of the depth estimates with GPR. One can improve the accuracy by measuring velocity of propagation of the electromagnetic waves through the firn using common-midpoint surveys (e.g. Brown *et al.* 2012b) and/or calibrations using water-level measurements in boreholes. During our fieldwork, we have observed that the water content in the firn varies seasonally and laterally, which would require rather frequent calibrations of GPR signals. However, errors in the water table measurement provided by GPR do not affect the MRS estimate of the water volume in firn, which was our principal target, but the time limitation for the entire survey imposed by weather conditions suggested simplifying the GPR fieldwork, thus accepting some additional inaccuracy.

The MRS water-volume estimates reported in this study have been carried out using the 1D assumption and, consequently, horizontal stratification of the subsurface. MRS provides an estimate of the water volume in a vertical column with the size of 1 × 1 × 40 m^3 (in our case, we assume no water below 40 m). Then, the water volume observed with MRS is a product of the water volume contained in one column with the surface area of 1 m^2 and the surface area where the horizontal stratification is valid. We do not use GPR results for improving MRS inversion for water volume because the uncertainty in the water table depth has little influence on the water-volume estimate with MRS (Legchenko *et al.* 2004). Our study is the first to use the MRS in Greenland (to our knowledge, the use of MRS in Greenland has not been reported in the literature). We expected the aquifer within the depth range of 5–20 m and used the NUMIS$^{\mathrm{LITE}}$ instrument designed for shallow investigations. With this equipment, the bottom of the aquifer located around 35 m deep was not well resolved with MRS. For comparison, we found similar depth ranges of the firn-aquifer bottom using seismic refraction surveys (28 ± 3 m) and borehole salt dilution tests (34 ± 5 m) done at similar location with the MRS (Miller *et al.* 2017; Montgomery *et al.* 2017). In the future, the resolution of the bottom can be improved using a fourfold more powerful MRS instrument (NUMIS$^{\mathrm{POLY}}$ fabricated by IRIS Instruments (http://www.iris-instruments.com/) or GMR of VISTA CLARA, Inc. (http://www.vista-clara.com/)). However, even with a more powerful system, the accuracy of the MRS method to determine the water table depth is not as good as the one provided by GPR (Legchenko and Shushakov 1998; Weichman *et al.* 2002; Müller-Petke and Yaramanci 2008; Parsekian and Grombacher 2015; Legchenko *et al.* 2017).

So far, only a few ice-sheet scale estimates of the water volume are available for the Greenland ice sheet. A water volume estimate of 2150 ± 105 kg m^{-3} was made for a 15-m-thick aquifer in Greenland (Koenig *et al.* 2014). This measurement falls in the upper end of our water volume estimates for the Helheim firn aquifer. On the other end, for a thin firn aquifer (1.25-m-thick) on South Cascade Glacier, Fountain (1988) reports a total volume of 115 kg m^{-3} stored in the firn. Other previous studies of firn aquifers on mountain glaciers, compiled in the review paper of Fountain and Walder (1998), do not always offer a direct water volume estimate.

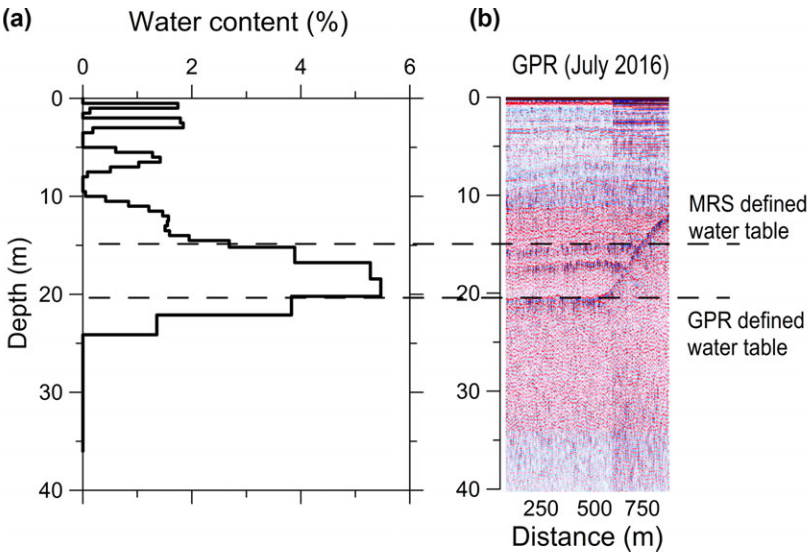

Figure 8 (a) MRS water content log; (b) corresponding GPR cross-section showing a multi-reflection response.

In addition, numerical regional models currently suffer the lack of accurate physics for the snow/firn model component, usually routing water in the snow vertically via a 1D bucket approach and holding water solely via capillary forces (e.g. Langen *et al.* 2017; Meyer and Hewitt 2017; Steger *et al.* 2017).

Therefore, independent direct water volume estimates with geophysical technics such as MRS will help guide model development and validate/calibrate numerical simulations. A joint use of GPR and MRS seems to provide a compromise between the information provided by these methods and the data production rate during fieldwork. One difficulty that should be resolved in the future is the absence of a quantitative calibration of MRS water estimates using other robust *in situ* measurements.

CONCLUSIONS

We report our experience of using magnetic resonance sounding (MRS) and ground-penetrating radar (GPR) methods for investigating the Greenland firn aquifer. Our results show that the MRS method is able to detect liquid water in the firn and provides an approximate location of water-saturated formations as well as an estimation of the water volume. MRS allows unambiguous identification of GPR reflections in term of the detection of the top of the aquifer. Thus, accuracy and high production rate of GPR are combined with the reliability of water identification with MRS. We consider MRS results as quantitative information, but the difficulty of applying the verification procedure under firn-aquifer conditions does not allow us to confirm MRS results by other *in situ* measurements.

Monitoring of the firn aquifer in Greenland carried out in 2015 and 2016 reveals an accumulation of water at an average depth between 20 and 30 m, thus confirming that the sensitivity of MRS is sufficient for following annual variations of water volume. MRS results suggest that at the monitoring test site, the volume of water stored in the firn increased approximately by 28% between April 2015 and late July 2016 corresponding to two melt seasons.

ACKNOWLEDGEMENTS

Our work was made possible with the financial support from a grant from Labex OSUG@2020 (Investissements d'avenir – grant # ANR10 LABX56). The authors also acknowledge the French National Program (ANR) 'Investment for Future - Excellency Equipment' project EQUIPEX CRITEX (grant #ANR-11-EQPX-0011) provided MRS equipment for the fieldwork. The field study in Greenland became possible due to financial support provided by the NSF (proposal number: NSF-PLR-1417987 and NSF-PLR-1417993). We acknowledge CH2MHILL Polar Services for organizing the field logistics and thank them for an outstanding support during the 2015 and 2016 expeditions.

REFERENCES

Arcone S., Lawson D. and Delaney A. 1995. Short-pulse radar wavelet recovery and resolution of dielectric contrasts within englacial and basal ice of Matanuska Glacier, Alaska, U.S.A. *Journal of Glaciology* **41**, 68–86.

Behroozmand A.A., Keating K. and Auken E. 2015. A review of the principles and applications of the NMR technique for near-surface characterization. *Surveys in Geophysics* **36**, 27–85.

Björnsson H., Gjessing Y., Hamran S., Hagen J., Liestøl O., Pálsson F. and Erlingsson B. 1996. The thermal regime of sub-polar glaciers mapped by multi-frequency radio-echo sounding. *Journal of Glaciology* **42**, 23–32.

Boucher M., Girard J.F., Legchenko A., Baltassat J.M., Dörfliger N. and Chalikakis K. 2006. Using magnetic resonance soundings to locate a water-filled karst conduit, *Journal of Hydrology* **330**, 413–421, https://doi.org/10.1016/j.jhydrol.2006.03.034.

Bradford J. and Harper J. 2005. Wave field migration as a tool for estimating spatially continuous radar velocity and water content in glaciers. *Geophysical Research Letters* **32**, https://doi.org/10.1029/2004GL021770.

Braun M. and Yaramanci U. 2008. Inversion of resistivity in magnetic resonance sounding. *Journal of Applied Geophysics* **66**, 151–164

Brown J.R., Brox T.I., Vogt S.J., Seymour J.D., Skidmore M.L. and Codd S.L. 2012. Magnetic resonance diffusion and relaxation characterization of water in the unfrozen vein network in polycrystalline ice and its response to microbial metabolic products. *Journal of Magnetic Resonance* **225**, 17–24.

Brown J., Bradford J., Harper J., Pfeffer W.T., Humphrey N. and Mosley-Thompson E. 2012b. Georadar-derived estimates of firn density in the percolation zone, western Greenland ice sheet: Georadar-derived firn density profiles. *Journal of Geophysical Research: Earth Surface* **117**, https://doi.org/10.1029/2011JF002089.

Brox T.I., Skidmore M.L. and Brown J.R. 2015. Characterizing the internal structure of laboratory ice samples with nuclear magnetic resonance. *Journal of Glaciology* **61**, 55–64, https://doi.org/10.3189/2015JoG14J133.

Callaghan P.T., Dykstra R., Eccles C.D., Haskell T.G. and Seymour J.D. 1999. A nuclear magnetic resonance study of Antarctic sea ice brine diffusivity. *Cold Regions Science and Technology* **29**, 153–171, https://doi.org/10.1016/S0165-232X(99)00024-5.

Chevalier A., Legchenko A., Girard J.F. and Descloitres M. 2014. 3D Monte Carlo inversion of magnetic resonance measurements. *Geophysical Journal International* **198**, 216–228, https://doi.org/10.1093/gji/ggu091.

Christianson K., Kohler J., Alley R.B., Nuth C. and van Pelt W.J.J. 2015. Dynamic perennial firn aquifer on an Arctic glacier. *Geophysical Research Letters* **42**, https://doi.org/10.1002/2014GL062806.

Endres A.L., Murray T., Booth A.D. and West L.J. 2009. A new framework for estimating englacial water content and pore geometry using combined radar and seismic wave velocities. *Geophysical Research Lettters* **36**, https://doi.org/10.1029/2008GL036876.

Fettweis X., Franco B., Tedesco M., van Angelen J.H., Lenaerts J.T.M., van den Broeke M.R. and Gallée H. 2013. Estimating the Greenland ice sheet surface mass balance contribution to future sea level rise using the regional atmospheric climate model MAR. *The Cryosphere* **7**, 469–489, https://doi.org/10.5194/tc-7-469-2013.

Forster R.R., Box J.E., Van den Broeke M.R., Miège C., Burgess E.W., Van Angelen J.H., Lenaerts J.T.M., Koenig L.S., Paden J., Lewis C., Gogineni S.P., Leuschen C. and McConnell J.R. 2014. Extensive liquid meltwater storage in firn within the Greenland ice sheet. *Nature Geoscience* **7**, 95–98, https://doi.org/10.1038/ngeo2043.

Fountain A.G. 1988. The storage of water in, and hydraulic characteristics of, the firn of South Cascade Glacier, Washington State, U.S.A. *Annals of Glaciology* **13**, 69–75.

Fountain A.G. and Walder J.S. 1998. Water flow through temperate glaciers. *Reviews of Geophysics* **36**, 299–328, https://doi.org/10.1029/97RG03579.

Garambois S., Legchenko A., Vincent C. and Thibert E. 2016. Ground-penetrating radar and surface nuclear magnetic resonance monitoring of an englacial water-filled cavity in the polythermal glacier of Tête Rousse. *Geophysics* **81**, WA131–WA146, https://doi.org/10.1190/GEO2015-0125.1.

Grombacher D., Fiandaca G., Behroozmand A.A. and Auken E. 2017. Comparison of stabiliser functions for surface NMR inversions. *Near Surface Geophysics* **15**, 533–544, https://doi.org/10.3997/1873-0604.2017027.

Guillen A. and Legchenko A. 2002a. Inversion of surface nuclear magnetic resonance data by an adapted Monte Carlo method applied to water resource characterization. *Journal of Applied Geophysics* **50**, 193–205.

Guillen A. and Legchenko A. 2002b. Application of linear programming techniques to the inversion of proton magnetic resonance measurements for water prospecting from the surface. *Journal of Applied Geophysics* **50**, 149–162.

Gusmeroli A., Murray T., Jansson P., Pettersson R., Aschwanden A. and Booth A. 2010. Vertical distribution of water within the polythermal Storglaciären, Sweden. *Journal of Geophysical Research* **115**, https://doi.org/10.1029/2009FJ001539.

Helm V., Humbert A. and Miller H. 2014. Elevation and elevation change of Greenland and Antarctica derived from CryoSat-2. *The Cryosphere* **8**, 1539–1559.

Hertrich M. 2008. Imaging of groundwater with nuclear magnetic resonance. *Progress in Nuclear Magnetic Resonance Spectroscopy* **53**, 227–248.

Hertrich M., Braun M., Gunther T., Green A.G. and Yaramanci U. 2007. Surface nuclear magnetic resonance tomography. *IEEE Transactions on Geoscience and Remote Sensing* **45**, 3752–3759, https://doi.org/10.1109/TGRS.2007.903829.

Hertrich M., Green A.G., Braun M. and Yaramanci U. 2009. High-resolution surface NMR tomography of shallow aquifers based on multioffset measurements. *Geophysics* **74**, G47–G59.

Hoekstra P. 1978. Electromagnetic methods for mapping shallow permafrost. *Geophysics* **43**, 782–787.

Irvine-Fynn T.D.L., Hodson A., Moorman B., Vatne G. and Hubbard A. 2011. Polythermal glacier hydrology. *A review: Reviews of Geophysics* **49**, https://doi.org/10.1029/2010RG000350.

Irvine-Fynn T.D.L., Moorman B.J., Williams J.L.M. and Walter F.S.A. 2006. Seasonal changes in ground-penetrating radar signature observed at a polythermal glacier, Bylot Island, Canada. *Earth Surface Processes and Landforms* **31**, 892–909.

Jiang C., Müller-Petke M., Lin J. and Yaramanci U. 2015. Imaging shallow three dimensional water-bearing structures using magnetic resonance tomography. *Journal of Applied Geophysics* **116**, 17–27.

Kneisel C. 2004. New insights into mountain permafrost occurrence and characteristics in glacier forefields at high altitude through the application of 2-D resistivity imaging. *Permafrost and Periglacial Processes* **15**, 221–227.

Koenig L.S., Miege C., Forster R.R. and Brucker L. 2014. Initial in situ measurements of perennial meltwater storage in the Greenland firn aquifer. *Geophysical Research Letters* **41**, 81–85.

Kovacs A., Gow A.J. and Morey R.M. 1995. The in-situ dielectric constant of polar firn revisited. *Cold Regions Science and Technology* **23**, 245–256.

Langen P.L., Fausto R.S., Vandecrux B., Mottram R.H. and Box J.E. 2017. Liquid water flow and retention on the Greenland ice sheet in the regional climate model HIRHAM5: local and large-scale impacts. *Frontiers in Earth Science* **4**, https://doi.org/10.3389/feart.2016.00110.

Legchenko A. 2013. Magnetic Resonance Imaging for Groundwater. Wiley-ISTE.

Legchenko A., Baltassat J.-M., Bobachev A., Martin C., Robin H. and Vouillamoz J.-M. 2004. Magnetic resonance sounding applied to aquifer characterization. *Journal of Groundwater* **42**, 363–373.

Legchenko A., Clément R., Garambois S., Maury E., Mic L-M., Laurent J-P., Desplanque C. and Guyard H. 2011a. Locating water storage of the Luitel lake peat bog using MRS, ERT and GPR. *Near Surface Geophysics* **9**, 201–209.

Legchenko A., Comte J.-C., Ofterdinger U., Vouillamoz J.-M., Lawson F.M.A. and Walsh J. 2017. Joint use of singular value decomposition and Monte-Carlo simulation for estimating uncertainty in surface NMR inversion. *Journal of Applied Geophysics* **144**, 28–36.

Legchenko A., Descloitres M., Vincent C., Guyard H., Garambois S., Chalikakis K. and Ezersky M. 2011b. Three-dimensional magnetic resonance imaging for groundwater. *New Journal of Physics* **13**, https://doi.org/10.1088/1367-2630/13/2/025022.

Legchenko A. and Pierrat G. 2014. Glimpse into the design of MRS instrument. *Near Surface Geophysics* **12**, 297–308.

Legchenko A. and Valla P. 2002. A review of the basic principles for proton magnetic resonance sounding measurements. *Journal of Applied Geophysics* **50**, 3–19.

Legchenko A., Vincent C., Baltassat J.M., Girard J.F., Thibert E., Gagliardini O., Descloitres M., Gilbert A., Garambois S., Chevalier A. and Guyard H. 2014. Monitoring water accumulation in a glacier using magnetic resonance imaging. *The Cryosphere* **8**, 155–166.

Legchenko A.V. and Shushakov O.A. 1998. Inversion of surface NMR data. *Geophysics* **63**, 75–84.

Lehmann-Horn J.A., Walbrecker J.O., Hertrich M., Langston G., McClymont A.F. and Green A.G. 2011. Imaging groundwater beneath a rugged proglacial moraine. *Geophysics* **76**, B165–B172.

Meyer C.R. and Hewitt I.J. 2017. A continuum model for meltwater flow through compacting snow. *The Cryosphere Discussions* 1–24, https://doi.org/10.5194/tc-2017-128.

Miège C., Forster R.R., Box J.E., Burgess E.W., Mcconnell J.R., Pasteris D.R. and Spikes V.B. 2013. Southeast Greenland high accumulation rates derived from firn cores and ground-penetrating radar. *Annals of Glaciology* **54**, https://doi.org/10.3189/2013AoG63A358.

Miège C., Forster R., Brucker L., Koenig L., Solomon D.K., Paden J., Box J., Burgess E., Miller J., McNerney L., Brautigam N., Fausto R. and Gogineni S.P. 2016. Spatial extent and temporal variability of Greenland firn aquifers detected by ground and airborne radars. *Journal of Geophysical Research, Earth Surface* **121**, https://doi.org/10.1002/2016JF003869.

Miller O., Solomon D.K., Miège C., Koenig L., Forster R., Schmerr N., Ligtenberg S. and Montgomery L. 2017. Direct evidence of meltwater flow within a firn aquifer in Southeast Greenland: meltwater flow within firn aquifer. *Geophysical Research Letters* https://doi.org/10.1002/2017GL075707.

Mohnke O. and Yaramanci U. 2002. Smooth and block inversion of surface NMR amplitudes and decay times using simulated annealing. *Journal of Applied Geophysics* **50**, 163–177.

Montgomery L.N., Schmerr N., Burdick S., Forster R.R., Koenig L., Legchenko A., Ligtenberg S., Miège C., Miller O.L. and Solomon D.K. 2017. Investigation of firn aquifer structure in Southeastern Greenland using active source seismology. *Frontiers in Earth Science* **5**, 10.

Moran M.L., Greenfield R.J. and Arcone S.A. 2000. Delineation of a complexly dipping temperate glacier bed using short-pulse radar arrays. *Journal of Glaciology* **46**, 274–286.

Morozov V.A. 1966. On the solution of functional equations by the method of regularization. *Soviet Mathematics - Doklady* **7**, 414–417.

Müller-Petke M. and Yaramanci U. 2008. Resolution studies for magnetic resonance sounding (MRS) using the singular value decomposition. *Journal of Applied Geophysics* **66**, 165–175.

Murray T., Booth A. and Rippin D. 2007. Water-content of glacier-ice: limitations on estimates from velocity analysis of surface ground-penetrating radar surveys. *Journal of Environmental and Engineering Geophysics* **12**, 87–99.

Murray T., Gooch D.L. and Stuart G.W. 1997. Structures within the surge front at Bakaninbreen Svalbard, using ground-penetrating radar. *Annals of Glaciology* **24**, 122–129.

Murray T., Stuart G.W., Fry M., Gamble N.H. and Crabtree M.D. 2000. Englacial water distribution in a temperate glacier from surface and borehole radar velocity analysis. *Journal of Glaciology* **46**, 389–398.

Nuber A., Rabenstein L., Lehmann-Horn J.A., Hertrich M., Hendricks S., Mahoney A. and Eicken H. 2013. Water content estimates of a first-year sea-ice pressure ridge keel from surface-nuclear magnetic resonance tomography. *Annals of Glaciology* **54**, 33–43.

Parsekian A.D. and Grombacher D. 2015. Uncertainty estimates for surface nuclearmagnetic resonance water content and relaxation time profiles from bootstrap statistics. *Journal of Applied Geophysics* **119**, 61–70.

Parsekian A.D., Grosse G., Walbrecker J.O., Müller-Petke M., Keating K., Liu L., Jones B.M. and Knight R. 2013. Detecting unfrozen sediments below thermokarst lakes with surface nuclear magnetic resonance. *Geophysical Research Letters* **40**, 535–540.

Pettersson R., Jansson P. and Holmlund P. 2003. Cold surface layer thinning on Storglaciären, Sweden, observed by repeated ground penetrating radar surveys. *Journal of Geophysical Research* **108**, https://doi.org/10.1029/2003JF000024.

Rennermalm A.K., Moustafa S.E., Mioduszewski J., Chu V.W., Forster R.R., Hagedorn B., Harper J.T., Mote T.L., Robinson D.A., Shuman C.A., Smith L.C. and Tedesco M. 2013. Understanding Greenland ice sheet hydrology using an integrated multiscale approach. *Environment Research Letters* **8**, https://doi.org/10.1088/1748-9326/8/1/015017.

Rippin D., Willis I., Arnold N., Hodson A., Moore J., Kohler J. and Bjornsson H. 2003. Changes in geometry and subglacial drainage of Midre Lovénbreen, Svalbard, determined from digital elevation models. *Earth Surface Processes and Landforms* **28**, 273–298.

Semenov A.G., Schirov M.D., Legchenko A.V., Burshtein A.I. and Pusep A.Yu. 1989. Device for measuring the parameter of underground mineral deposit. G.B. Patent 2198540B.

Steger C.R., Reijmer C.H., van den Broeke M.R., Wever N., Forster R.R., Koenig L.S., Kuipers Munneke P., Lehning M., Lhermitte S., Ligtenberg S.R.M., Miege Clement and Noël, B.P.Y. 2017. Firn meltwater retention on the Greenland ice sheet: a model comparison. *Frontiers in Earth Science* **5**, 1–16.

Tikhonov A. and Arsenin V. 1977. Solution of Ill-Posed Problems. John Wiley & Sons.

Turu V. 2012. Surface NMR survey on Hansbreen Glacier, Hornsund, SW Spitsbergen (Norway). *Landform Analysis* **21**, 57–74.

Vincent C., Descloitres M., Garambois S., Legchenko A., Guyard H., Lefebvre E. and Gilbert A. 2012. Detection of a subglacial lake in Glacier de Tete Rousse (Mont Blanc area, France). *Journal of Glaciology* **58**, 866–878.

Weichman P.B., Lun D.R., Ritzwoller M.H. and Lavely E. 2002. Study of surface nuclearmagnetic resonance inverse problems. *Journal of Applied Geophysics* **50**, 129–147.